

Optimized SC-F-LOAM: Optimized Fast LiDAR Odometry and Mapping Using Scan Context

Lizhou Liao, Chunyun Fu*, Binbin Feng, and Tian Su

Abstract— LiDAR odometry can achieve accurate vehicle pose estimation for short driving range or in small-scale environments, but for long driving range or in large-scale environments, the accuracy deteriorates as a result of cumulative estimation errors. This drawback necessitates the inclusion of loop closure detection in a SLAM framework to suppress the adverse effects of cumulative errors. To improve the accuracy of pose estimation, we propose a new LiDAR-based SLAM method which uses F-LOAM as LiDAR odometry, Scan Context for loop closure detection, and GTSAM for global optimization. In our approach, an adaptive distance threshold (instead of a fixed threshold) is employed for loop closure detection, which achieves more accurate loop closure detection results. Besides, a feature-based matching method is used in our approach to compute vehicle pose transformations between loop closure point cloud pairs, instead of using the raw point cloud obtained by the LiDAR sensor, which significantly reduces the computation time. The KITTI dataset and a UGV platform are used for verifications of our method, and the experimental results demonstrate that the proposed method outperforms typical LiDAR odometry/SLAM methods in the literature. Our code is made publicly available for the benefit of the community¹.

Index Terms— LiDAR Odometry, Loop Closure Detection, Global Optimization, SLAM

I. INTRODUCTION

Simultaneous localization and mapping (SLAM) plays an important role in the fields of robotics and autonomous driving; it also lays the foundation for path planning and motion control of robots and driverless vehicles [1]. According to different sensors used, SLAM solutions can be roughly classified into two major types: LiDAR SLAM and visual SLAM. Compared with cameras, LiDAR sensors are advantageous in measurement accuracy, measurement range, and resistance to environmental interference, which makes LiDAR SLAM generally more accurate in localization [2]. So far, LiDAR SLAM has been widely adopted in the fields of robotics and autonomous driving.

A. Literature Review

LiDAR SLAM has undergone more than 30 years' development. Up to now, a large number of LiDAR SLAM-related works have been published in the literature.

This work was supported by the National Natural Science Foundation of China under Grant 51805055. (corresponding author: Chunyun Fu)

Lizhou Liao, Binbin Feng and Tian Su are with the College of Mechanical and Vehicle Engineering, Chongqing University, Chongqing 400044, China. E-mail: {lizolizhou, fengbinbin, sutian}@cqu.edu.cn.

Chunyun Fu is with the State key Laboratory of Mechanical transmission and the College of Mechanical and Vehicle Engineering, Chongqing University, Chongqing 400044, China. E-mail: fuchunyun@cqu.edu.cn.

¹ <https://github.com/SlamCabbage/Optimized-SC-F-LOAM>

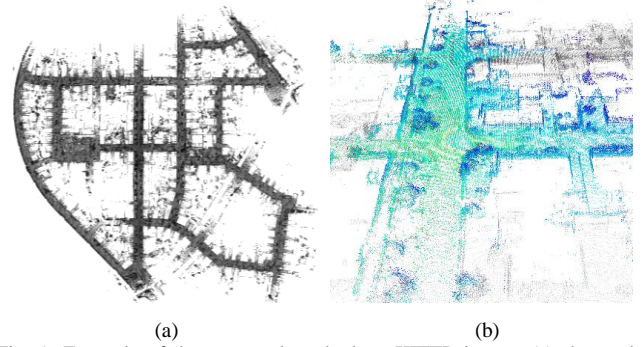


Fig. 1: Example of the proposed method on KITTI dataset. (a) shows the mapping effect of the proposed method on KITTI dataset sequence 00. (b) shows an instance of loop closure detection, where the colored part is the point cloud in the current frame and the gray part is the historical map.

Solutions to SLAM problems have also evolved from statistical-based approaches in early years [3] to graph optimization methods nowadays [4]. In the last decade, typical LiDAR SLAM solutions have developed into a framework containing three major parts, including front-end odometry, loop closure detection and global optimization [5-7].

Frame matching is the most central task for front-end odometry in LiDAR SLAM, where estimation of vehicle/robot pose transformation between two consecutive frames is performed. The accuracy of frame matching determines the overall vehicle/robot pose estimation accuracy, while the frame-matching efficiency determines the real-time performance of LiDAR SLAM. Frame matching generally includes raw point cloud matching and feature-based matching. For raw point cloud matching, the most classical method is Iterative Closest Point (ICP) [8] which finds the closest point in Euclidean space for each point in the other point cloud, iteratively minimizes this distance residual and converges to the final estimated pose. However, ICP requires costly computation due to the huge number of points. Another common method for raw point cloud matching is the Normal Distribution Transformation (NDT) [9] which puts the point cloud data into grids and then calculates the local normal distribution in each grid, so as to reduce the computational cost of iteration by point-to-normal distribution matching. However, the matching accuracy with NDT is dependent on grid size, and it deteriorates in case of large grids. Zhang and Singh [10] proposed a feature-based inter-frame matching method known as Lidar Odometry and Mapping (LOAM), which has become a benchmark inter-frame matching method up to now. In this method, feature points (edge points and plane points) are extracted based on local point smoothness, and the feature points extracted from the current frame are matched with corresponding established feature submap to

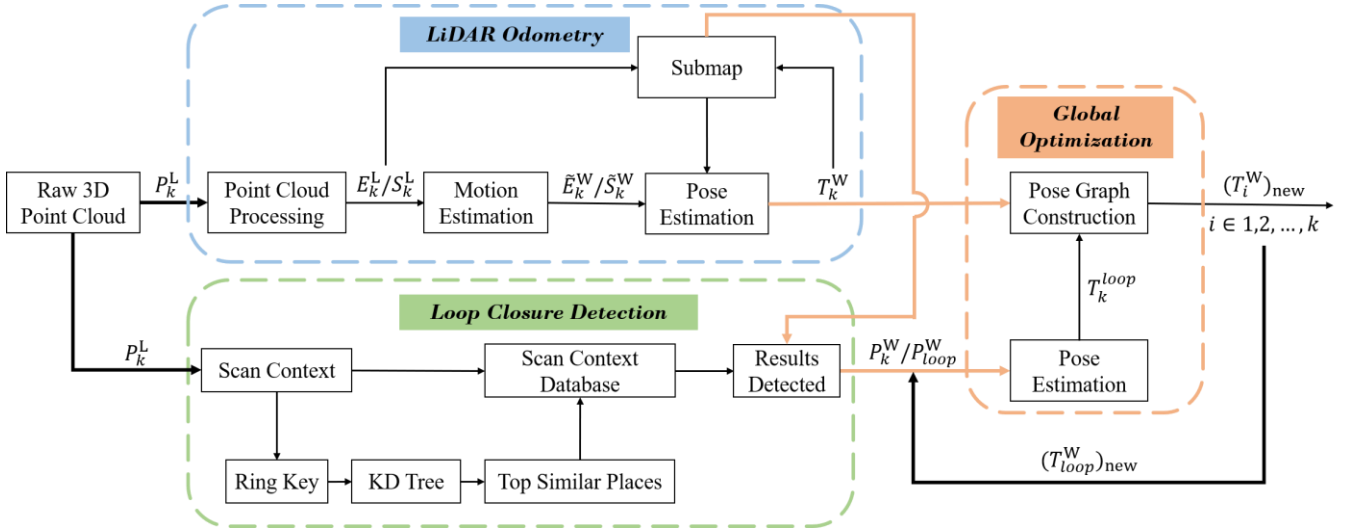


Fig. 2. Schematic of the Simple-SC-F-LOAM. The three different-colored dashed boxes represent three parallel processing modules. The blue dashed box represents the LiDAR odometry module, the green one represents the loop closure detection module, and the orange one represents the global optimization module.

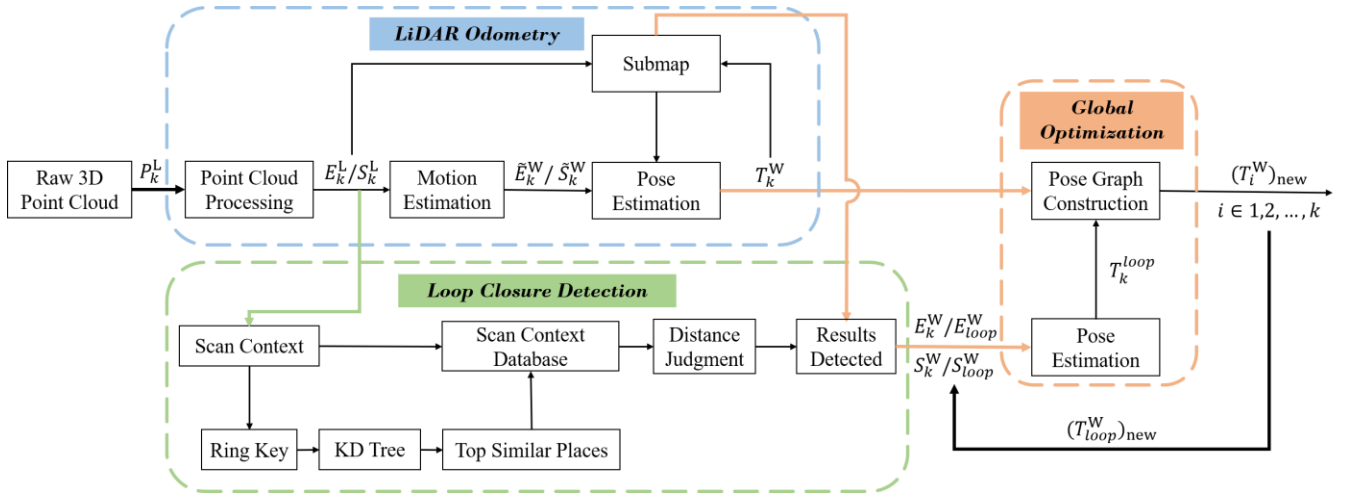


Fig. 3. Schematic of the proposed Optimized-SC-F-LOAM. The three different-colored dashed boxes represent three parallel processing modules. The blue one represents the LiDAR odometry module, the green one represents the loop closure detection module, and the orange one represents the global optimization module.

obtain the pose transformation. Based on Ceres Solver [11], Wang et al. [2] proposed Fast LiDAR Odometry and Mapping (F-LOAM), which further optimizes the frame matching accuracy of LOAM and reduces the computational cost. The pose estimation accuracy of F-LOAM is ranked among the best according to the KITTI odometry benchmark [12]; yet presence of cumulative error due to its lack of loop closure detection reduces its effectiveness in large-range estimation scenarios.

As for loop closure detection, a number of vision-based solutions have been proposed in the literature, such as [13-15]. These loop detection methods are subject to many limitations as a result of poor robustness to ambient illumination [16]. Although the loop closure detection concept is widely used in visual SLAM, applications of the same concept to LiDAR SLAM still remain a challenge. LiDAR-based loop closure detection methods can be categorized broadly into local descriptor methods and global descriptor methods. The former

ones relate to calculating the location signatures of detected key points, constructing a bag-of-words model, and finally matching the location signatures with those of other frames to obtain the similarity between them [17-20]. This category of methods has unstable performance in matching local key points in outdoor scenarios where unstructured objects (e.g., trees) are present and in cases where point cloud density varies with distance. To solve this problem, global descriptor methods were subsequently proposed in the literature. Kim and Kim [21] put forward a global descriptor method to reduce the dimensionality of a frame of point cloud data and store such data in a two-dimensional matrix. The row of the matrix represents the distance of a partitioned ground area (i.e. a bin) to the LiDAR center, and the column represents the angle of this bin relative to the x -direction. Then the global descriptor of the current frame is used to derive the similarity with those of other frames and finally the loop closure detection result. Dube et al. [22] proposed a segmentation-based scene recognition method, known as SegMatch. Firstly, the raw

point cloud is segmented into several clusters, and one



Fig. 4. UGV platform.

descriptor is extracted from each cluster. Then, Random Forest Classifier [23] is employed to predict the similarity of one point cloud cluster with other clusters, and the historical frames which satisfy the similarity threshold condition are identified. Lastly, RANSAC [24] is used for geometric verification, in order to derive the loop closure detection result and the pose transformation between the matched frames. This SegMatch method has been used as the loop closure detection module in [25, 26] to achieve global optimization of vehicle pose. However, additional point cloud processing is required in [25, 26], which increases the computational cost of loop closure detection.

For global optimization, the most common approach is pose graph optimization [27]. Several popular open source C++ libraries [11, 28, 29] can be used to solve global optimization problems, among which GTSAM [28] archives good optimization result at low computational cost [30]. For this reason, GTSAM is used in the present study for global optimization.

B. Problem statement

In the existing literature, many LiDAR SLAM methods have only front-end odometry without loop closure detection [2, 10, 31-34]. As a result, vehicle/robot pose estimation errors accumulate as the explored scene expands. Although some LiDAR SLAM methods in the recent literature [25, 26, 35] have incorporated loop closure detection, most of them constructed pose constraints by simply including one loop closure method in the SLAM framework, which does not necessarily guarantee optimal localization accuracy.

SC-LeGO-LOAM, a combination of LeGO-LOAM [32] and Scan Context [21], is able to achieve global optimization of vehicle pose upon loop closure and thereby reduce the accumulated errors. However, the ICP algorithm [8] adopted in SC-LeGO-LOAM for computing the pose transformation between loop closure point cloud pairs requires costly computation and may affect real-time establishment of loop constraints. F-LOAM [2] is a lightweight LiDAR odometry method with greatly reduced computational cost, but it is unable to achieve accurate localization in large scenarios due to lack of loop closure detection that can reduce the cumulative pose estimation error. Therefore, it is highly necessary to improve integration of LiDAR odometry and

loop closure detection, mainly because 1) reducing the cumulative error in pose estimation leads to improved SLAM accuracy; 2) lowering the cost of calculating pose transformation between loop closure point cloud pairs lightens the workload of the SLAM method.

C. Original Contribution

To solve the above problems, a lightweight LiDAR SLAM method, i.e. Optimized Fast LiDAR Odometry and Mapping Using Scan Context (Optimized-SC-F-LOAM), is proposed in this paper, based on F-LOAM [2] and Scan Context [21]. The Optimized-SC-F-LOAM method comprises three parts: LiDAR odometry, loop closure detection and global optimization; it can be used to achieve more accurate localization at less computational cost. Main contributions of this paper are as follows:

1. F-LOAM is optimized using Scan Context, thereby improving the localization accuracy in large scenes.

2. Feature-based matching method is used, instead of the conventional raw point cloud matching (such as ICP), to calculate the pose transformation between loop closure point cloud pairs, which significantly reduces the computational cost.

3. An adaptive distance threshold is employed to identify whether a loop closure is established. This threshold reduces the possibility of false loop closure detection and further improves the localization accuracy. Moreover, due to reduced false loop closure detections, the computation time of global optimization is also shortened.

4. The entire SLAM framework is made publicly available for the benefit of the community under appropriate license agreement.

To demonstrate advantages of the proposed method, we have compared the proposed algorithm based on the commonly used KITTI dataset [36] with a direct combination of Scan Context and F-LOAM. The results show that the method proposed in this paper provides higher localization accuracy and lower computational cost compared to Simple-SC-F-LOAM. The details of Simple-SC-F-LOAM are given in Section II.

D. Outline of Paper

The remainder of the paper is organized as follows: Section II introduces the method for comparison in this paper; Section III explains the proposed method in detail, including LiDAR odometry, loop closure detection and global optimization; Section IV provides the comparative experimental results and discussions on results; Section V summarizes the whole paper.

II. BACKGROUND

In this paper, we name the direct combination of F-LOAM [2] and Scan Context [21] as Simple-SC-F-LOAM. The specific framework of Simple-SC-F-LOAM is shown in Fig. 2. In this framework, the 3D raw point cloud p_k^l is passed into the LiDAR Odometry module and the Loop Closure Detection module to derive the vehicle pose T_k^w in the current frame relative to the global coordinate system, as well as the loop closure detection result. If a loop closure is detected, the pose

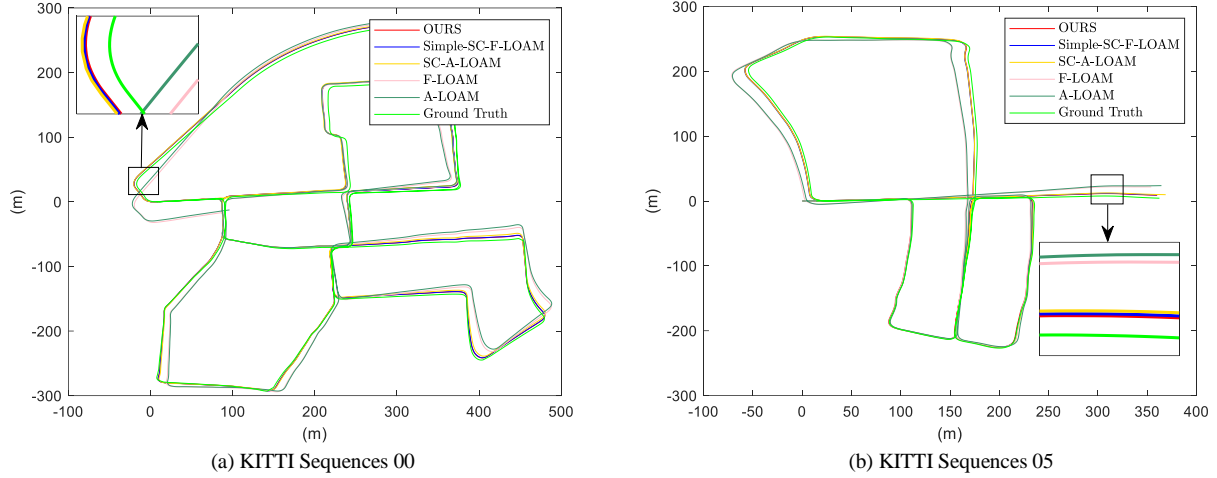


Fig. 5. Comparison of trajectories on KITTI dataset: (a) and (b) are the trajectories produced by all competing methods using KITTI sequences 00 and 05.

TABLE I. Results on KITTI Sequence 00 and Sequence 05.

Methods	Datasets	ATE (%)	ARE (deg/100m)	Time (ms/loop frame)
Simple-SC-F-LOAM	00	0.75	0.27	501
	05	0.51	0.24	422
F-LOAM	00	1.13	0.37	-
	05	0.81	0.32	-
SC-A-LOAM	00	0.83	0.34	444
	05	0.50	0.27	439
A-LOAM	00	1.09	0.40	-
	05	0.87	0.37	-
LeGO-LOAM	00	2.17	13.4	-
	05	1.28	0.74	-
LOAM	00	0.78	-	-
	05	0.57	-	-
OURS	00	0.75	0.27	135
	05	0.43	0.22	129

T_{loop}^w , resulting from the LiDAR odometry is used to transform the loop closure point cloud pair to the same coordinate system, leading to p_k^w and p_{loop}^w . Then, the vehicle pose transformation T_k^{loop} between the point cloud pair p_k^w and p_{loop}^w is calculated using the ICP algorithm, and it is added to the pose graph together with the odometry pose T_k^w . Lastly, global optimization is performed to obtain the optimized vehicle pose.

According to the test based on the KITTI dataset [36], Simple-SC-F-LOAM can provide satisfactory localization accuracy. However, this method uses ICP to calculate the vehicle pose transformation between a loop closure point cloud pair, and as a result, the computation load significantly increases when encountered consecutive loop closures and loop constraints cannot be added to the pose graph in real time. Real tests have proved that the method proposed in this work takes merely 28% of the time required on average by Simple-SC-F-LOAM to compute the pose transformation

between a loop closure point cloud pair. Besides, the original Scan Context method results in many false loop closure detections that not only increase the computational cost but also reduce the accuracy of final vehicle localization. To tackle this false detection problem, the proposed method is designed with an adaptive distance threshold that can eliminate most false loop closure detections resulting from Scan Context, thereby improving the accuracy of vehicle localization.

III. METHODOLOGY

In this section, the proposed SLAM method is elaborated. The entire framework of the method proposed in this paper is shown in Fig. 3. Similar to that of Simple-SC-F-LOAM, the framework of the proposed method also consists of three modules: LiDAR Odometry, Loop Closure Detection and Global Optimization, but it differs in the following three aspects:

1. Feature point clouds obtained by the LiDAR odometry are used as the input to the Loop Closure Detection module.

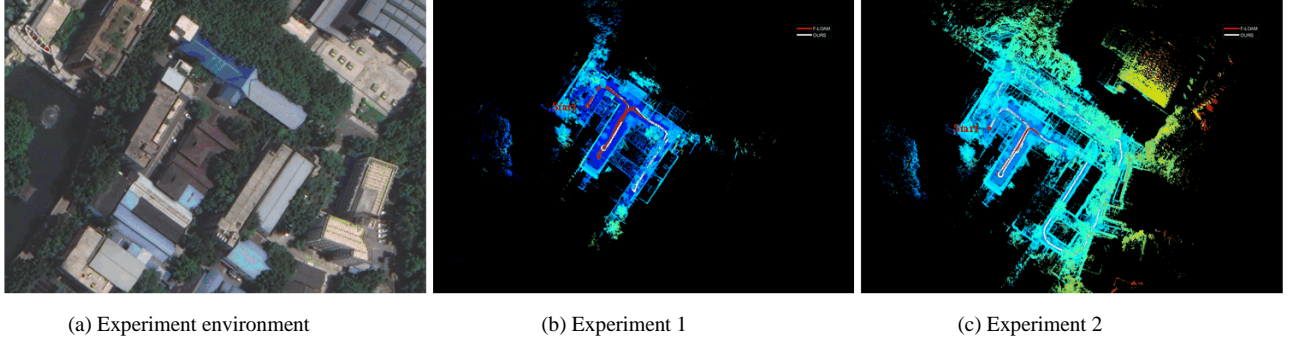


Fig. 6. Experiment environment of the UGV platform.

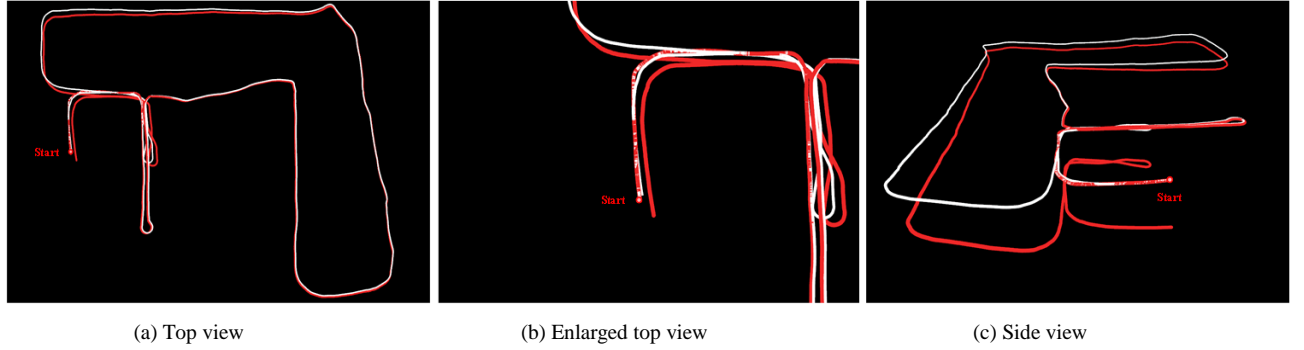


Fig. 7. Trajectories produced by F-LOAM and our method in experiment 2: The trajectory obtained by our method is in white, and that by F-LOAM is in red.

2. An adaptive distance threshold is used to identify whether a loop closure is established, so as to reduce false loop closure detections.

3. Feature-based matching is employed to compute the vehicle pose transformation between a loop closure point cloud pair.

A. LiDAR Odometry

In the LiDAR Odometry module, a framework substantively consistent with [2] is employed. This LiDAR odometry mainly includes four sub-modules: 1) Point Cloud Processing, 2) Motion Estimation, 3) Pose Estimation and 4) Submap Update. These sub-modules are introduced one by one below.

1) Point Cloud Processing: This sub-module in the LiDAR odometry first receives the raw point cloud data collected by LiDAR, and uses the same method as described in [2, 10, 32] to extract feature points based on local point smoothness. Specifically, the smoothness of each point is compared with the smoothness threshold. A point with smoothness greater than the threshold is considered as an edge point, otherwise it is deemed as a plane point. Then, the edge point cloud E_k^L formed by all edge points and the plane point cloud S_k^L formed by all plane points are passed to the Motion Estimation sub-module and the Submap Update sub-module.

2) Motion Estimation: The Motion Estimation sub-module in the LiDAR odometry receives the incoming edge point cloud E_k^L and plane point cloud S_k^L , and uses the uniform

motion model [2] to estimate the initial pose transformation from the LiDAR coordinate system in the current frame to the global coordinate system. By means of this initial pose transformation, the edge point cloud E_k^L and the plane point cloud S_k^L are transformed into the global coordinate system to obtain \tilde{E}_k^W and \tilde{S}_k^W , which are then passed into the Pose Estimation sub-module.

3) Pose Estimation: This sub-module receives the edge point cloud \tilde{E}_k^W and the plane point cloud \tilde{S}_k^W in the global coordinate system, and the feature submap passed in from the Submap Update sub-module. Firstly, 5 adjacent points corresponding to each feature point in the feature submap are identified. Then, the adjacent points of the edge feature points form corresponding feature lines, and the adjacent points of the plane feature points form corresponding feature surfaces. The sum of all distances from feature points to corresponding feature lines (or feature surfaces) forms a nonlinear equation. Secondly, the Gauss-Newton nonlinear optimization method is used to iteratively solve pose transformation T_k^W from the current frame to the global coordinate system. For specific optimization steps, please refer to [2]. Lastly, T_k^W is passed into the Submap Update sub-module to update the feature submap, and simultaneously into the Global Optimization module to build the pose graph.

4) Submap Update: This sub-module receives the feature point clouds E_k^L and S_k^L in the current frame, and the pose transformation T_k^W from the LiDAR coordinate system in the

current frame to the global coordinate system. Then, E_k^L and S_k^L are projected via T_k^W to the global coordinate system and added to the feature map for use by the Pose Estimation sub-module in the next frame.

B. Loop Closure Detection

The Loop Closure Detection module of the proposed method has incorporated the well-known Scan Context framework [21]. For brevity, the details of Scan Context are not repeated and we hereby introduce the major differences between the proposed method and the original Scan Context.

A loop closure detection framework usually constructs a global descriptor for detection using the input point clouds. Different from Scan Context which uses raw point cloud data to form the global descriptor, the proposed method constructs the global descriptor using the edge point cloud E_k^L and the plane point cloud S_k^L obtained from the LiDAR Odometry module. These two types of feature points, E_k^L and S_k^L , contain almost all useful information in the point cloud raw data. The use of these feature points reduces the influence of clutters, improves the accuracy of loop closure detection, and shortens the loop closure detection time.

The original Scan Context method uses a fixed distance threshold to determine and exclude highly similar but far-away point cloud pairs. As a result, setting a large fixed distance threshold may cause many false loop closure detections. To overcome this shortcoming, in this study we have introduced an adaptive distance threshold to replace the conventional fixed distance threshold. By this means, false loop closure detections can be reduced. Once the loop closure detection results are obtained, we use the poses T_k^W and T_{loop}^W corresponding to the loop closure point cloud pair to calculate the distance between the two frames, as follows:

$$\tilde{T}_k^{loop} = T_{loop}^W \cdot T_k^W \quad (1)$$

$$d = \sqrt{\tilde{T}_k^{loop} \cdot x()^2 + \tilde{T}_k^{loop} \cdot y()^2 + \tilde{T}_k^{loop} \cdot z()^2} \quad (2)$$

where \tilde{T}_k^{loop} represents the pose transformation between the current frame and the loop frame obtained through the LiDAR odometry results T_k^W and T_{loop}^W , $\tilde{T}_k^{loop} \cdot x()$, $\tilde{T}_k^{loop} \cdot y()$, and $\tilde{T}_k^{loop} \cdot z()$ denote the x , y , and z components of the vector connecting the preceding two frames (i.e. pointing from the current frame to the loop frame), and d is the magnitude of this vector. If d is greater than a certain threshold d_{thre} , then it is considered that no loop closure is detected.

Since the cumulative error increases with the distance traveled by the vehicle, we design the threshold d_{thre} as a function of the number of odometry frames:

$$d_{thre} = 20 + k / 100 \quad (3)$$

where k represents the number of odometry frames. This threshold can reduce false loop closure detections, thereby improving global optimization results and efficiency of the entire SLAM algorithm.

C. Global Optimization

Reducing the cumulative error in vehicle pose estimation is a frequently discussed issue in the existing literature. The global optimization method used in this paper consists of two main sub-modules: 1) Pose Estimation and 2) Pose Graph Construction.

1) The Pose Estimation sub-module receives loop closure detection results from the Loop Closure Detection module, and based on such results, it obtains point clouds of the current frame and the loop frame in the global coordinate system from the LiDAR Odometry module. It should be noted that for computation of vehicle pose transformation between a loop closure point cloud pair, these two point cloud frames that constitute a loop closure must be in the same coordinate system [21]. For this purpose, we first project the current frame to the global coordinate system based on $(T_{loop}^W)_{new}$ (which will be explained in the next paragraph), and construct a submap of the loop-frame point cloud and its neighbors in the global coordinate system. Then, we use the pose estimation method in the LiDAR Odometry module to calculate the pose transformation T_k^{loop} between the current-frame point cloud and the submap so constructed, and pass this pose transformation to the Pose Graph Construction sub-module for constructing the pose graph.

2) The Pose Graph Construction sub-module receives the pose transformation T_k^{loop} passed in by the Pose Estimation sub-module and the pose transformation T_k^W passed in by the LiDAR Odometry module. The received odometry pose T_k^W is added to its corresponding pose graph node, and pose T_k^{loop} is added as the edge corresponding to the node. Following that, the GTSAM algorithm [28] is used for global optimization of the pose graph to derive the optimized pose $(T_i^W)_{new}$, $i \in 1, 2, \dots, k$.

IV. EXPERIMENT EVALUATION

A. Experiment Setup

To validate the effectiveness of our method in real scenes, we tested our method in gentle outdoor scenes and undulating outdoor scenes. For tests in the gentle outdoor scene, we adopted sequences 00 and 05 from the KITTI dataset [36] for evaluation. For tests in the undulating outdoor scene, we used the point cloud collected by a UGV platform (see Fig. 4) inside the university campus. All tests were done based on the Robot Operating System (ROS) that was installed on a laptop with an AMD R5-5600H processor, a 16 GB RAM and the Ubuntu platform.

B. Evaluation on KITTI dataset

We used the open source KITTI dataset to test the performance of the proposed algorithm in gentle outdoor scenes. Since the proposed method is mainly intended to optimize pose estimation by LiDAR odometry under the condition of loop scenes, the sequences 00 and 05 in the KITTI dataset which contain loop closures were used to evaluate the localization accuracy and computational efficiency of the proposed method. For comparison purposes, the proposed method is compared against some typical LiDAR SLAM methods in the literature [2, 10, 21, 32] by using the same data sequences.

Fig. 5 shows the trajectories of the proposed method, the compared methods [2, 10, 21, 32] and the ground truths. We see that for both sequences, the proposed method outperforms the competing methods by providing trajectories closest to the ground truths. We also computed the Average Translational Error (ATE), the Average Rotational Error (ARE), and the computation time between loop closure point cloud pairs in these two sequences for each method. Table I shows that the proposed method has the smallest ATE and ARE for both sequences. At the same time, the proposed method also achieves the optimal computation time for both sequences. Specifically, for sequence 00, the time consumed by the proposed method is 73.1% and 69.6% less than those of Simple-SC-F-LOAM and SC-A-LOAM, respectively. As for sequence 05, the time consumed by the proposed method is 69.4% and 70.6% lower than those of Simple-SC-F-LOAM and SC-A-LOAM, respectively. Note that the ATE and ARE produced by LeGO-LOAM and LOAM were directly obtained from [33], and other results were computed by the authors using the source codes provided by the competing methods, on the same testing laptop as described above.

C. Experiment with measured dataset

We performed comparative tests (i.e. experiment 1 and experiment 2) of the proposed method with F-LOAM [2] by using real scene data collected by a UGV equipped with a 16-beam LiDAR. Fig. 6(a) shows the top view of the real scene in the university campus. Fig. 6(b) shows a loop closure part in this scene with a relatively slight slope and the trajectories generated by the two methods. Fig. 6(c) shows a larger loop closure part in the same scene and the trajectories produced by the two methods, which contains a larger slope compared to that in Fig. 6(b). In Figs. 7(a) and 7(b), we see that our method closes the loop better than F-LOAM in the X - Y plane, while the trajectory generated by F-LOAM deviates to some extent. Fig. 7(c) shows that F-LOAM produces a more pronounced deviation in the z -axis direction, while our method can still successfully close the loop. The above results indicate that our method can achieve better localization in the case of loops with large gradient changes.

D. Discussions on results

To sum up, in the slight-slope scene, the proposed method has achieved great improvements in aspects of computation time and localization accuracy relative to the compared methods. There are two main reasons for these improvements. One is that feature point matching (instead of ICP matching) is used in the proposed method to calculate the vehicle pose transformation between loop closure point cloud pairs, thereby reducing the computation time. The other is that a loop judgment criterion is re-adaptively designed in the proposed method for loop closure detection with Scan Context to reduce false loop closure detections, so that a more accurate pose can be obtained after global optimization. In the large-slope scene, the proposed method outperforms F-LOAM in terms of localization accuracy especially in the z -axis direction, due to the incorporation of loop closure detection in our method for suppressing the cumulative pose estimation errors.

V. CONCLUSION

In this paper, a computationally efficient LiDAR-based SLAM framework is proposed, which achieves better localization and mapping results at a lower computational cost. By combining a currently efficient LiDAR odometry method (F-LOAM) with a LiDAR loop closure detection method (Scan Context), the proposed method is designed with an adaptive distance threshold (instead of a fixed threshold) for loop closure detection, thereby optimizing loop closure detection performance. Such design has enabled the proposed method to achieve better localization accuracy and much higher computational efficiency.

In order to validate the effectiveness of the proposed method, we used the real scene dataset - KITTI dataset and the point cloud data collected by a UGV for comparative tests with several typical SLAM approaches in the literature. The results show that the proposed method outperforms the compared methods in terms of localization accuracy and computation time of pose transformation between loop closure point cloud pairs.

REFERENCES

- [1] A. K. Gostar et al., "State Transition for Statistical SLAM Using Planar Features in 3D Point Clouds," (in English), *Sensors-Basel*, vol. 19, no. 7, p. 1614, Apr 3 2019, doi: 10.3390/s19071614.
- [2] W. H. W. C. C. C. and X. L., "F-LOAM : Fast LiDAR Odometry and Mapping," in 2021 IEEE/RSJ International Conference on Intelligent Robots and Systems (IROS), 2021.
- [3] H. Durrant-Whyte and T. Bailey, "Simultaneous localization and mapping: part I," *IEEE robotics & automation magazine*, vol. 13, no. 2, pp. 99-110, 2006.
- [4] D. Koller and N. Friedman, *Probabilistic graphical models: principles and techniques*. MIT press, 2009.
- [5] H. Wang, C. Wang, and L. Xie, "Intensity-slam: Intensity assisted localization and mapping for large scale environment," *IEEE Robotics and Automation Letters*, vol. 6, no. 2, pp. 1715-1721, 2021.
- [6] L. Li et al., "SA-LOAM: Semantic-aided LiDAR SLAM with Loop Closure," in 2021 IEEE International Conference on Robotics and Automation (ICRA), 2021: IEEE, pp. 7627-7634.
- [7] J. Jiang, J. Wang, P. Wang, P. Bao, and Z. Chen, "LiPMatch: LiDAR point cloud plane based loop-closure," *IEEE Robotics and Automation Letters*, vol. 5, no. 4, pp. 6861-6868, 2020.
- [8] P. J. Besl and N. D. McKay, "Method for registration of 3-D shapes," in *Sensor fusion IV: control paradigms and data structures*, 1992, vol. 1611: International Society for Optics and Photonics, pp. 586-606.
- [9] P. Biber and W. Straßer, "The normal distributions transform: A new approach to laser scan matching," in *Proceedings 2003 IEEE/RSJ International Conference on Intelligent Robots and Systems (IROS 2003)*(Cat. No. 03CH37453), 2003, vol. 3: IEEE, pp. 2743-2748.
- [10] J. Zhang and S. Singh, "LOAM: Lidar Odometry and Mapping in Real-time," in *Robotics: Science and Systems*, 2014, vol. 2, no. 9.
- [11] S. Agarwal and K. Mierle, "Ceres solver: Tutorial & reference," Google Inc, vol. 2, no. 72, p. 8, 2012.
- [12] A. Geiger, P. Lenz, and R. Urtasun, "Are we ready for autonomous driving? the kitti vision benchmark suite," in 2012 IEEE conference on computer vision and pattern recognition, 2012: IEEE, pp. 3354-3361.
- [13] M. Cummins and P. Newman, "FAB-MAP: Probabilistic localization and mapping in the space of appearance," *The International Journal of Robotics Research*, vol. 27, no. 6, pp. 647-665, 2008.
- [14] A. Angeli, D. Filliat, S. Doncieux, and J.-A. Meyer, "Fast and incremental method for loop-closure detection using bags of visual words," *IEEE transactions on robotics*, vol. 24, no. 5, pp. 1027-1037, 2008.
- [15] D. Gálvez-López and J. D. Tardos, "Bags of binary words for fast place recognition in image sequences," *IEEE Transactions on Robotics*, vol. 28, no. 5, pp. 1188-1197, 2012.

- [16] C. Valgren and A. J. Lilienthal, "Sift, surf and seasons: Long-term outdoor localization using local features," in 3rd European conference on mobile robots, ECMR'07, Freiburg, Germany, September 19-21, 2007, 2007, pp. 253-258.
- [17] B. Steder, M. Ruhnke, S. Grzonka, and W. Burgard, "Place recognition in 3D scans using a combination of bag of words and point feature based relative pose estimation," in 2011 IEEE/RSJ International Conference on Intelligent Robots and Systems, 2011: IEEE, pp. 1249-1255.
- [18] Y. Zhong, "Intrinsic shape signatures: A shape descriptor for 3d object recognition," in 2009 IEEE 12th International Conference on Computer Vision Workshops, ICCV Workshops, 2009: IEEE, pp. 689-696.
- [19] I. Sipiran and B. Bustos, "A Robust 3D Interest Points Detector Based on Harris Operator," in 3DOR@ Eurographics, 2010, pp. 7-14.
- [20] B. Steder, R. B. Rusu, K. Konolige, and W. Burgard, "NARF: 3D range image features for object recognition," in Workshop on Defining and Solving Realistic Perception Problems in Personal Robotics at the IEEE/RSJ Int. Conf. on Intelligent Robots and Systems (IROS), 2010, vol. 44.
- [21] G. Kim and A. Kim, "Scan context: Egocentric spatial descriptor for place recognition within 3d point cloud map," in 2018 IEEE/RSJ International Conference on Intelligent Robots and Systems (IROS), 2018: IEEE, pp. 4802-4809.
- [22] R. Dube, D. Dugas, E. Stumm, J. Nieto, and C. Cadena, "SegMatch: Segment based place recognition in 3D point clouds," in 2017 IEEE International Conference on Robotics and Automation (ICRA), 2017.
- [23] L. Breiman, "Random forests," *Machine learning*, vol. 45, no. 1, pp. 5-32, 2001.
- [24] M. A. Fischler and R. C. Bolles, "Random sample consensus: a paradigm for model fitting with applications to image analysis and automated cartography," *Communications of the ACM*, vol. 24, no. 6, pp. 381-395, 1981.
- [25] X. Ji, L. Zuo, C. Zhang, and Y. Liu, "Lloam: Lidar odometry and mapping with loop-closure detection based correction," in 2019 IEEE International Conference on Mechatronics and Automation (ICMA), 2019: IEEE, pp. 2475-2480.
- [26] X. Liu, L. Zhang, S. Qin, D. Tian, and C. Chen, "Optimized LOAM Using Ground Plane Constraints and SegMatch-Based Loop Detection," *Sensors*, vol. 19, no. 24, p. 5419, 2019.
- [27] F. Lu and E. Milios, "Globally consistent range scan alignment for environment mapping," *Autonomous robots*, vol. 4, no. 4, pp. 333-349, 1997.
- [28] F. Dellaert, "Factor graphs and GTSAM: A hands-on introduction," Georgia Institute of Technology, 2012.
- [29] G. Grisetti, R. Kümmerle, H. Strasdat, and K. Konolige, "g2o: A general framework for (hyper) graph optimization," in Proceedings of the IEEE International Conference on Robotics and Automation (ICRA), Shanghai, China, 2011, pp. 9-13.
- [30] A. dela Juric, F. Kendeš, I. Markovic, and I. Petrovic, "A Comparison of Graph Optimization Approaches for Pose Estimation in SLAM."
- [31] S. W. Chen et al., "Sloam: Semantic lidar odometry and mapping for forest inventory," *IEEE Robotics and Automation Letters*, vol. 5, no. 2, pp. 612-619, 2020.
- [32] T. Shan and B. Englot, "Lego-loam: Lightweight and ground-optimized lidar odometry and mapping on variable terrain," in 2018 IEEE/RSJ International Conference on Intelligent Robots and Systems (IROS), 2018: IEEE, pp. 4758-4765.
- [33] X. Zheng and J. Zhu, "Efficient LiDAR Odometry for Autonomous Driving," *IEEE Robotics and Automation Letters*, vol. 6, no. 4, pp. 8458-8465, 2021, doi: 10.1109/LRA.2021.3110372.
- [34] S. Liang, Z. Cao, C. Wang, and J. Yu, "A Novel 3D LiDAR SLAM Based on Directed Geometry Point and Sparse Frame," *IEEE Robotics and Automation Letters*, vol. 6, no. 2, pp. 374-381, 2020.
- [35] J. Yin, Y. Zhang, and X. Li, "Added the Odometry Optimized SLAM Loop Closure Detection System," in 2020 5th International Conference on Control, Robotics and Cybernetics (CRC), 2020: IEEE, pp. 216-220.
- [36] A. Geiger, P. Lenz, C. Stiller, and R. Urtasun, "Vision meets robotics: The kitti dataset," *The International Journal of Robotics Research*, vol. 32, no. 11, pp. 1231-1237, 2013.